

This is the accepted manuscript made available via CHORUS. The article has been published as:

First identification of excited states in ^{117}Ba using the recoil- β -delayed proton tagging technique

B. Ding, Z. Liu, D. Seweryniak, P. J. Woods, H. L. Wang, J. Yang, H. L. Liu, C. N. Davids, M. P. Carpenter, T. Davinson, R. V. F. Janssens, R. D. Page, A. P. Robinson, J. Shergur, S. Sinha, S. Zhu, X. D. Tang, J. G. Wang, T. H. Huang, W. Q. Zhang, M. D. Sun, X. Y. Liu, and H. Y. Lu

Phys. Rev. C **95**, 024301 — Published 1 February 2017

DOI: [10.1103/PhysRevC.95.024301](https://doi.org/10.1103/PhysRevC.95.024301)

First identification of excited states in ^{117}Ba using the recoil- β -delayed proton tagging technique

B. Ding,¹ Z. Liu,^{1,*} D. Seweryniak,^{2,†} P. J. Woods,³ H. L. Wang,⁴ J. Yang,⁴ H. L. Liu,⁵ C. N. Davids,² M. P. Carpenter,² T. Davinson,³ R. V. F. Janssens,² R. D. Page,⁶ A. P. Robinson,² J. Shergur,⁷ S. Sinha,² S. Zhu,² X. D. Tang,¹ J. G. Wang,¹ T. H. Huang,¹ W. Q. Zhang,¹ M. D. Sun,^{1,8,9} X. Y. Liu,^{1,8} and H. Y. Lu^{1,8}

¹*Institute of Modern Physics, Chinese Academy of Sciences, Lanzhou 730000, China*

²*Argonne National Laboratory, Argonne, Illinois 60439, USA*

³*University of Edinburgh, Edinburgh, EH9 3JZ, United Kingdom*

⁴*Zhengzhou University, Zhengzhou 450001, China*

⁵*Xi'an Jiaotong University, Xi'an 710049, China*

⁶*University of Liverpool, Liverpool, L69 7ZE, United Kingdom*

⁷*University of Maryland, College Park, Maryland 20742, USA*

⁸*University of Chinese Academy of Sciences, Beijing 100049, China*

⁹*Lanzhou University, Lanzhou 730000, China*

(Dated: Received: January 18, 2017)

Excited states have been observed for the first time in the neutron-deficient nucleus ^{117}Ba using the Recoil-Decay Tagging technique following the heavy-ion fusion-evaporation reaction $^{64}\text{Zn}(^{58}\text{Ni}, 2p3n)^{117}\text{Ba}$. Prompt γ rays have been assigned to ^{117}Ba through correlations with β -delayed protons following the decay of $A = 117$ recoils. Through the analysis of the γ - γ coincidence relationships, a high-spin level scheme consisting of two bands has been established in ^{117}Ba . Based on the systematics of the level spacings in the neighboring barium isotopes, the two bands are proposed to have $\nu h_{11/2}[532]5/2^-$ and $\nu d_{5/2}[413]5/2^+$ configurations, respectively. The observed band-crossing properties are interpreted in the framework of cranked shell model.

PACS numbers: 21.10.Re, 23.20.-g, 23.20.Lv, 27.60.+j

I. INTRODUCTION

The evolution of quadrupole deformation and the presence of the octupole collectivity in the barium isotopes have attracted much attention both experimentally and theoretically [1–6]. As expected, quadrupole deformation was found to increase gradually with decreasing neutron number from the spherical $N = 82$ semi-magic nucleus ^{138}Ba to the $N = 66$ midshell isotope ^{122}Ba . These isotopes have been well studied with in-beam γ -ray spectroscopy and heavy-ion fusion-evaporation reactions, and a variety of structural features have been revealed. For example, at low rotational frequencies, the nuclear shape is strongly influenced by the opposite shape-driving forces of valence nucleons in the $h_{11/2}$ orbital [7]. At higher frequencies, competing rotation alignments between $\pi h_{11/2}$ and $\nu h_{11/2}$ nucleons have been observed [2, 8]. At even higher spins, collective excitations give way to quasiparticle excitations leading to band termination [9, 10]. On the other hand, the light isotopes with $Z \approx N \approx 56$ were predicted to be candidates for enhanced octupole collectivity [1, 11]; evidence for strong octupole correlations was observed in the neutron-deficient nuclei $^{112,114-117}\text{Xe}$ [12–15] and $^{118,122-125}\text{Ba}$ [3, 4, 16, 17]. Hence, it is of particular interest to extend spectroscopy studies toward more neutron-

deficient nuclei in this region and approach the $Z = N$ line as much as possible.

Experimentally such studies are challenging because the fusion-evaporation production cross sections for more neutron-deficient barium isotopes decrease rapidly, as charged-particle emission becomes dominant. Therefore, efficient exit channel selection is indispensable, as exemplified in the study of excited states in $^{120,121,122}\text{Ba}$ [2, 18, 19]. Taking advantage of the large γ -detector array Gammasphere [20] and the recoil mass separator FMA [21], high-spin states in $^{118,119}\text{Ba}$ were investigated by means of γ -recoil and Kx-ray- γ coincidence measurements.

For the most neutron-deficient nuclei, the Recoil-Decay Tagging (RDT) technique has been used to perform in-beam measurements [22]. In this method, charged-particle decay modes, such as α , proton, and superallowed β -ray emission, as well as isomeric decay provide highly selective tagging of the prompt γ rays from a nucleus of interest. Beta-delayed proton (βp) emission is one of the tagging methods and it has been successfully applied in the study of single neutron states outside doubly-magic ^{100}Sn where one γ ray was identified [23]. In an earlier study of ^{109}Te , singles γ -ray spectra (Figs. 5b and 5c in Ref. [22]) were obtained using βp together with α decays; a preliminary level scheme was proposed actually based on the recoil- γ - γ data, e.g., γ rays depopulating high-spin states could not tagged by recoil decay. In the present work, through the recoil- βp decay tagging, excited states in ^{117}Ba have been identified and furthermore, a high-spin level scheme has been established for the first time. Prior to this work, no

*Electronic address: liuzhong@impcas.ac.cn

†Electronic address: seweryniak@anl.gov

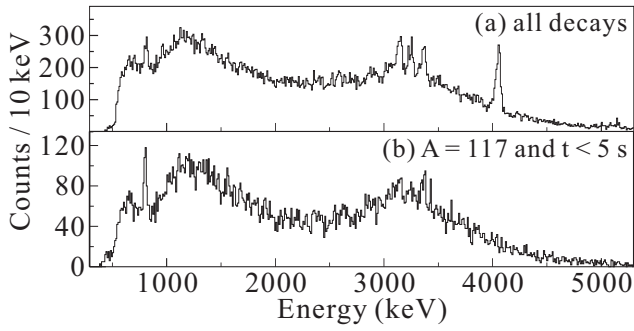


FIG. 1: Energy spectra (a) of all decays measured in the DSSD and (b) of decays from $A = 117$ residues within 5 s of implantation.

excited states were known in ^{117}Ba ; only the decay of the ground state was studied [24–26]. The ground state of ^{117}Ba was proposed to have $I^\pi = 3/2^+$ spin-parity from βp decay measurements with a decay branch of $\sim 16\%$ [26]. Its half-life was determined to be 1.75 s [24]. The preliminary results of this work were briefly presented in conference proceedings [27].

II. EXPERIMENT AND RESULTS

The experiment was performed at Argonne National Laboratory. High-spin states in ^{117}Ba were populated with the fusion-evaporation reaction $^{64}\text{Zn}(^{58}\text{Ni}, 2p3n)^{117}\text{Ba}$. The ^{58}Ni beam, with an energy of 305 MeV, was provided by the Argonne Tandem Linac Accelerator System (ATLAS). The target was a self-supporting, isotopically enriched, ^{64}Zn foil with a thickness of 0.7 mg/cm². It was irradiated for about 5 days with an average beam intensity of 5 pA. Prompt γ rays were detected by the Gammasphere array consisting of 100 Compton suppressed HPGe detectors [20]. The recoiling reaction products were separated from the unreacted beam and dispersed according to their mass-to-charge ratio A/q by the fragment mass analyser (FMA) [21]. The recoil's position at the FMA focal plane was measured in a parallel-grid avalanche counter (PGAC) followed by an ionization chamber (IC) used for energy loss measurements. Recoils with mass $A = 117$ and charge states $q = 27$ and 28 were selected through two mass slits optimised for the transmission of ^{117}La [28]. After passing through the PGAC and IC, the recoils were implanted into a 60 μm -thick double-sided silicon detector (DSSD) consisting of 80, 400 μm wide orthogonal strips on the front and rear, respectively, forming 6400 pixels. Following implantation, the recoils decayed in the pixel where they were implanted. Through spatial and temporal correlations, the decays were associated with individual implants. With the trigger condition of two or more Ge detector signals measured in coincidence with each other, or one or more Ge signals in coincidence with a PGAC event, approximately 1.1×10^6 events were recorded.

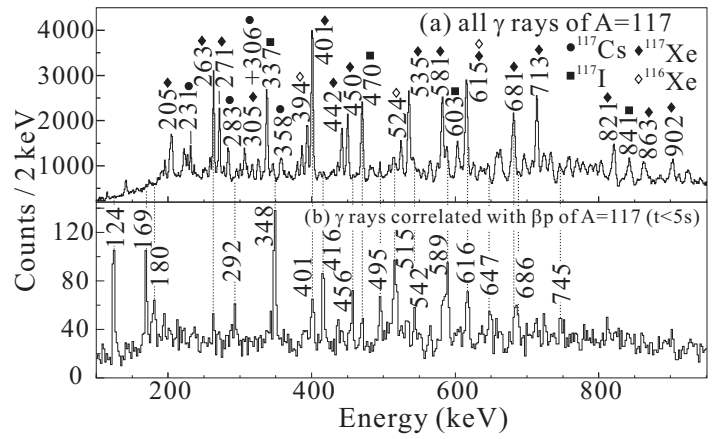


FIG. 2: Singles γ -ray spectra (a) gated on $A = 117$ residues and (b) tagged by βp -delayed proton decay from $A = 117$ recoils within 5 s of implantation.

The energy spectra of all the charged-particle decays and of those from $A = 117$ residues within 5 s of implantation are presented in Figs. 1a and 1b, respectively. In the figure, the broad bump around 3.2 MeV is from βp -delayed protons (βps) while the one around 1.2 MeV is from the escaping βps . A peak with an energy of ~ 800 keV belongs to the ground-state proton emitter ^{117}La with $T_{1/2} = 20.1(25)$ ms [28]. A γ -ray spectrum gated on $A = 117$ residues is presented in Fig. 2a, where the strong transitions from ^{117}Cs (231, 283, 306 keV, etc.), ^{117}Xe (263, 401, 535, 581, 713 keV, etc.), and ^{117}I (337, 470 keV, etc.) are dominant. Among these $A = 117$ isobars, besides ^{117}Ba , only ^{117}Xe , with $T_{1/2} = 61(2)$ s for the ground state, has a measurable βp branch with a ratio of $2.9(6) \times 10^{-5}$ [29]. By gating on the βps in the energy range of 1.2–3.2 MeV within 5 s of the implantation of $A = 117$ isobars, the strong γ rays present in the upper panel disappear or become much weaker. Thus the transitions present in the lower panel (Fig. 2b) mostly belong to ^{117}Ba .

In order to establish the ^{117}Ba level scheme, a γ - γ coincidence matrix was created by gating on βps within 5 s of the implantation of $A = 117$ recoils. The coincidence data were analyzed with the RADWARE software package [30]. From the detailed analysis of the γ - γ coincidence relationships, relative intensities, and γ -ray energy sums, a level scheme was established; it is presented in Fig. 3. Representative coincidence spectra demonstrating the existence of the two bands are found in Figs. 4 and 5. The level scheme consists of two independent rotational bands, labeled as band 1 and 2 in Fig. 3; no linking transitions between them were observed. The spins and parities of the two bands are tentatively assigned based on the level systematics in odd- A barium isotopes (see Fig. 6 and Sec. III). The γ -ray energies, relative intensities, and the proposed spins and parities are summarized in Table I.

The $\alpha = -1/2$ signature of the negative-parity band 1

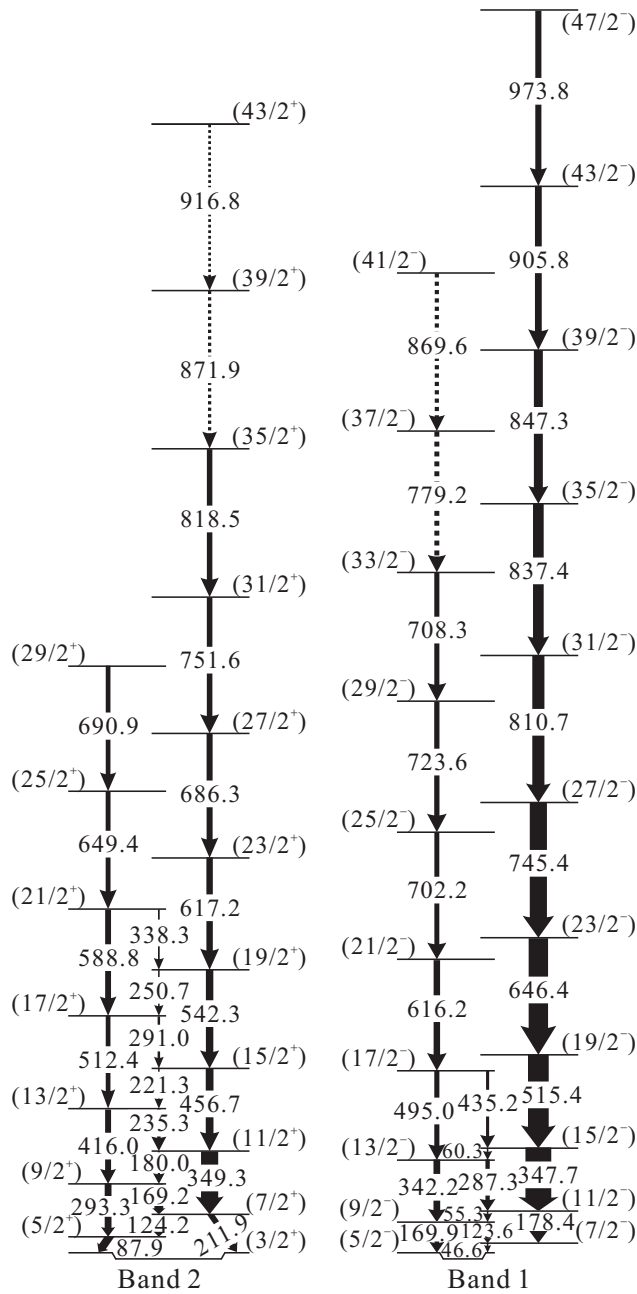


FIG. 3: Level scheme of ^{117}Ba proposed in this work.

is populated most strongly. In this branch, the ordering of the 178.4- and 347.7-keV transitions can be firmly established by the observation of the inter-signature $\Delta I = 1$ transitions; the ordering of the other eight transitions above the $I^\pi = 15/2^-$ level is proposed tentatively, based on relative intensities (see Table I). The $\alpha = 1/2$ signature of band 1, which was not presented in the preliminary results [27], is now firmly established, through the identification of some weak crossover or doublet transitions and their proper placement in the level scheme. The 124-, 170-, and 617-keV lines are all found to be doublets; the 123.6-, 169.9-, and 616.2-keV transitions were

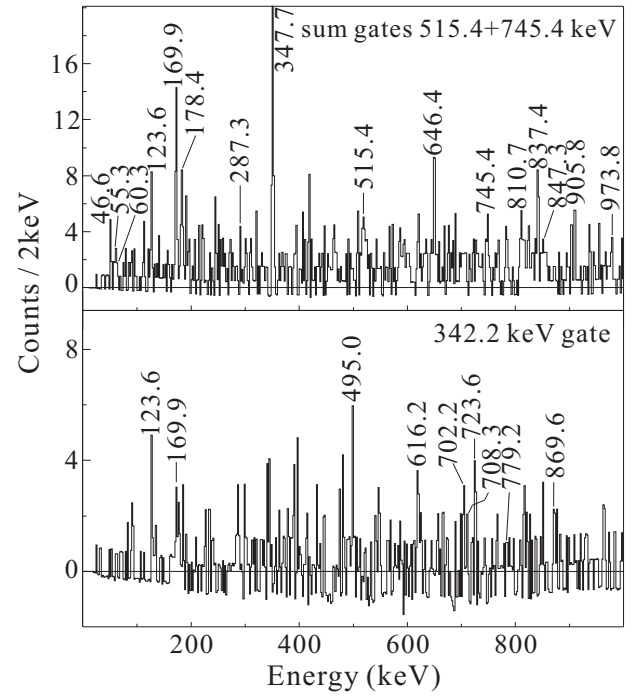


FIG. 4: Representative coincidence spectra with gates placed on selected transitions in band 1.

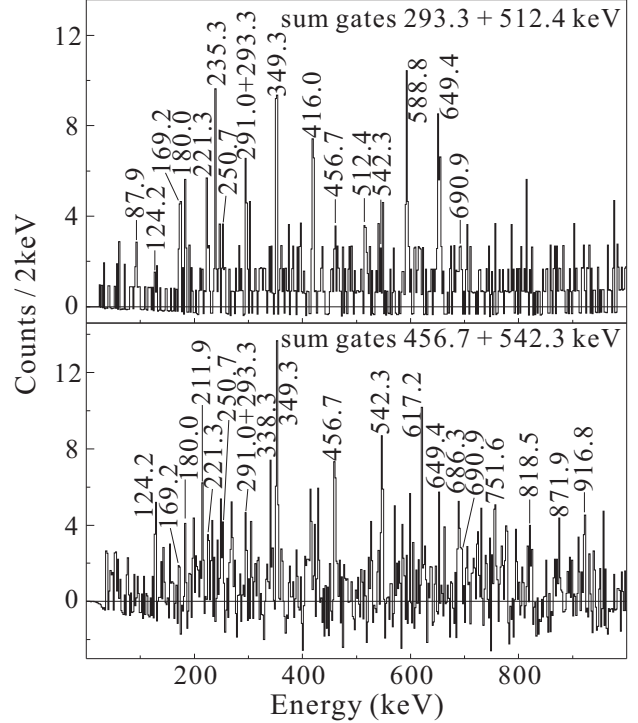


FIG. 5: Representative coincidence spectra with gates placed on selected transitions in band 2.

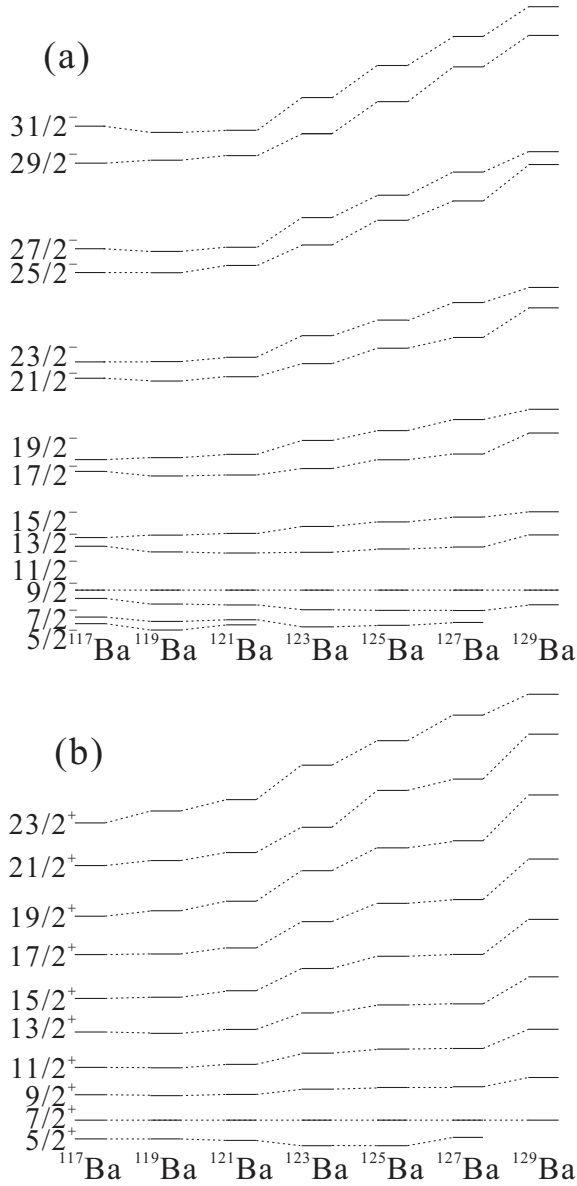


FIG. 6: Level-spacing systematics for (a) negative- and (b) positive-parity bands in the odd-A $^{117-129}\text{Ba}$ isotopes. The energies are normalized to the respective $11/2^-$ ($7/2^+$) states of negative-parity (positive-parity) bands. The data are from Refs. [8, 9, 17, 18, 35, 36] and the present work.

assigned in band 1 and the 124.2-, 169.2-, and 617.2-keV ones were placed in band 2. The ordering of the 495.0-, 342.2-, 169.9-keV cascade was determined unambiguously by the observation of the linking transitions between the two signatures in band 1. The ordering of the other γ rays in this sequence is based on their intensities. Apart from the negative-parity band, a positive-parity band (band 2) consisting of two $\Delta I = 2$ sequences was also established. In the lower part of band 2, the two signature sequences are inter-linked by $\Delta I = 1$ transitions.

The spin and parity of the ^{117}Ba ground state was

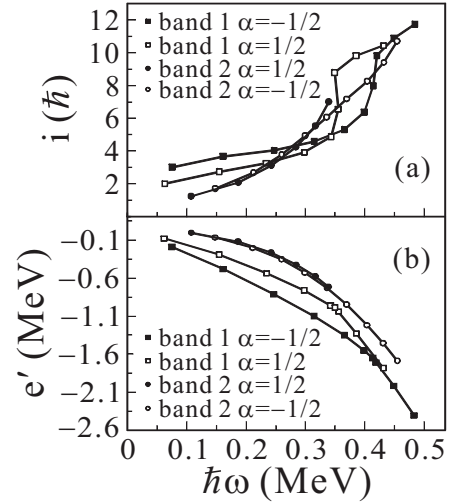


FIG. 7: (a) Extracted alignments and (b) Routhian energies for the ^{117}Ba rotational bands.

assigned as $I^\pi = 3/2^+$ in the βp decay measurement by means of a total absorption γ -ray spectrometer [26]. In the present work, γ rays were tagged with the βps . Therefore, it is tentatively proposed that the $I^\pi = 3/2^+$ state connected with band 2 is the $3/2^+$ ground state. However, the excitation energy for the states in band 1 cannot be determined, since the relative position of the two bands could not be established, as a situation similar to that occurring in ^{119}Ba [9]. It is noted that the intensity of the $7/2^+ \rightarrow 3/2^+$ transition is much weaker than that of the inband $15/2^+ \rightarrow 11/2^+$ one, indicating that the 211.9-keV transition does not belong to this positive-parity band and the $I^\pi = 3/2^+$ state has a different configuration as discussed in the following section. The 211.9- and 87.9-keV transitions are thus presented as out of band transitions in Fig. 3.

III. DISCUSSION

In ^{117}Ba ($N = 61$), the neutron Fermi surface lies between the $\nu g_{7/2}/d_{5/2}$ orbitals and the lower part of the $\nu h_{11/2}$ subshell. Collective bands based on these orbitals have been observed at low excitation energy in most nuclei in this region. Due to the high-j nature of the $\nu h_{11/2}$ orbital, bands built on them are strongly populated and become yrast in these nuclei. The relative excitation energies of the $\nu h_{11/2}$ bands in odd-A $^{119-129}\text{Ba}$ are plotted together with band 1 in Fig. 6a. Band 1 follows the systematic trend of the $\nu h_{11/2}$ bands so well that it most likely has the same origin. This assignment is supported further by the rotational properties of band 1 discussed below. It can be noticed in Fig. 6a that the lowest states in the $\nu h_{11/2}$ bands of $^{117,119,121}\text{Ba}$ are all characterised by $I^\pi = 5/2^-$ value, suggesting that they can all be associated with the same $\nu h_{11/2}[532]5/2^-$ configuration as proposed in Refs. [9, 31] for $^{119,121}\text{Ba}$.

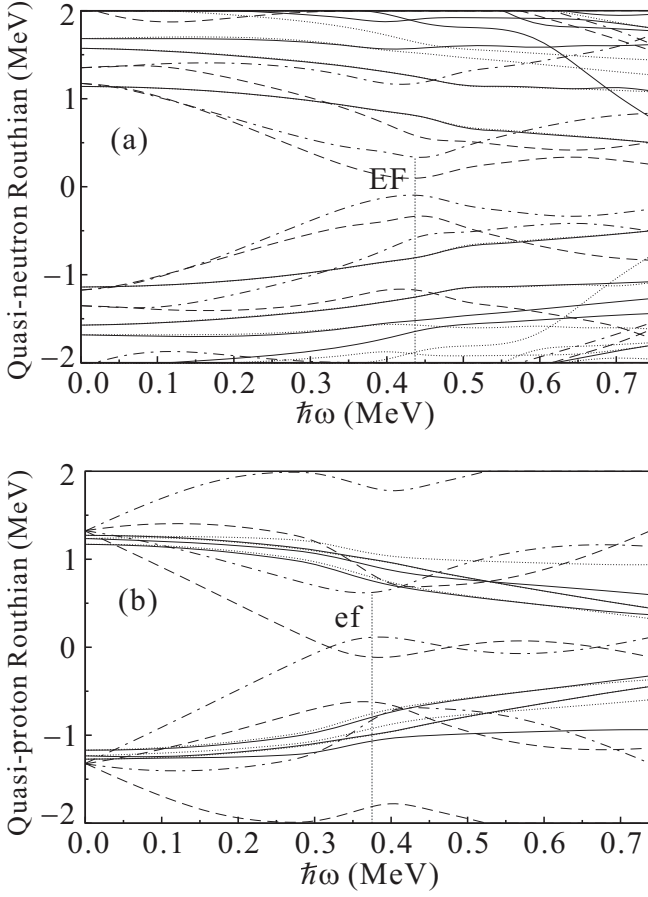


FIG. 8: Calculated quasiparticle Routhians for (a) neutrons and (b) protons as a function of rotational frequency ($\hbar\omega$). The deformation used in the calculations are give in the text. The different line styles represent values of parity and signature, (π, α) , as follows: dashed lines $(-, -1/2)$; dot-dashed lines $(-, +1/2)$; solid lines $(+, +1/2)$; and dotted lines $(+, -1/2)$. The lowest neutron and proton Routhians with $\alpha = +1/2$ and $\alpha = -1/2$ are both the $h_{11/2}$ orbitals. The positions of the lowest alignments for neutrons, e.g., EF in panel (a) and protons, e.g., ef in panel (b) are marked by faint vertical dotted lines.

Similarly, Fig. 6b indicates that band 2 follows the systematics of the positive-parity sequences in heavier odd-A Ba isotopes. However, as pointed out previously in Refs. [9, 31], such a comparison of the excitation energies for positive-parity states should be considered with caution, since the configurations of the corresponding bands change from the $\nu g_{7/2}$ to the $\nu d_{5/2}$ orbital with decreasing neutron number. Indeed, the positive-parity bands in odd-A $^{123-129}\text{Ba}$ were proposed to be associated with a $\nu g_{7/2}[404]7/2^+/[402]5/2^+$ configuration [32–35], while those in $^{119,121}\text{Ba}$ were assigned to be built predominantly on the $\nu d_{5/2}[413]5/2^+$ orbital [9, 18, 31]. This configuration change from $[402]5/2^+$ in ^{123}Ba to $[413]5/2^+$ in ^{121}Ba was confirmed by a laser spectroscopy measurement [37, 38], and results from the shift of the Fermi level. In ^{117}Ba , with two neutrons fewer than ^{119}Ba , the

$d_{5/2}[413]5/2^+$ configuration can be assigned to band 2, as discussed later. The experimental $B(M1)/B(E2)$ ratios for this band have been extracted. The error bars are rather large due to very low statistics, thus making a firm configuration assignment impossible. However, the average $B(M1)/B(E2)$ value over seven states in this band prefers a $\nu d_{5/2}$ rather than $\nu g_{7/2}$ configuration. Such a high-K configuration could account for the presence of strong inter-band $\Delta I = 1$ transitions and for a small signature splitting (see Fig. 7b). Although it should be kept in mind that strong configuration mixing between the $g_{7/2}[402]5/2^+$ and $d_{5/2}[413]5/2^+$ orbitals is anticipated and the configuration given above should be viewed as the predominant component of the wave function.

The level spacings in bands 1 and 2 (Fig. 6) decrease gradually with decreasing neutron number, indicating an increase in collectivity (deformation). The lowest levels are found either in ^{117}Ba (for example the $I^\pi = 15/2^-$ and $19/2^-$ levels) or in ^{119}Ba (for example the $I^\pi = 9/2^+$ and $11/2^+$ states) suggesting that the quadrupole deformation reaches a maximum between the two nuclei, e.g. in ^{118}Ba , consistent with various theoretical calculations (see e.g. Fig. 1 in Ref. [6]).

In order to investigate further the rotational properties of the two bands in ^{117}Ba , the experimental aligned angular momenta i_x and Routhians e' were extracted according to Ref. [39]: these are presented in Fig. 7. The Harris parameters [40] $J_0 = 17.0 \hbar^2 \text{MeV}^{-1}$ and $J_1 = 25.8 \hbar^4 \text{MeV}^{-3}$ were used to describe the energy of the rotating core. These values are the same as those used for other nuclei in this mass region [9, 31]. Backbends are clearly observed in band 1: the unfavored $\alpha = +1/2$ sequence experiences a band crossing at $\hbar\omega = 0.35 \text{ MeV}$ while the favored $\alpha = -1/2$ one, with a somewhat larger initial alignment, exhibits a smoother upbend at a slightly higher crossing frequency $\hbar\omega \approx 0.41 \text{ MeV}$. The total aligned angular momentum gain is $\sim 6.5 \hbar$ for both signatures. In the Routhian plot, it can be seen that the two signatures experience an energy splitting that increases gradually with frequency before the band crossing, and subsequently, after the crossing decreases rapidly before disappearing altogether. In band 2, the two signatures show an almost identical behavior with a small energy splitting. They also experience a gradual gain in alignment, indicating a strong band interaction. The $\alpha = +1/2$ signature experiences an upbend at $\hbar\omega \simeq 0.35 \text{ MeV}$ while the alignment frequency cannot be clearly determined in the $\alpha = -1/2$ signature. For both signatures, the band crossing is not yet completed over the frequency range observed in the present experiment.

To gain a qualitative insight into the structure of the low-lying states in ^{117}Ba , potential energy surface (PES) calculations were performed with the configuration-constrained blocking method [41]. The PES for one-quasineutron configurations were calculated in the three-dimensional $(\beta_2, \beta_4, \gamma)$ deformation space. Among the negative-parity configurations, the $\nu h_{11/2}[532]5/2^-$ one was found to be the lowest, supporting the configuration

assignment for band 1 proposed above. The two lowest positive-parity configurations were calculated to be $\nu g_{7/2}[411]3/2^+$ and $\nu d_{5/2}[413]5/2^+$. The potential minimum of the former is found to be very close to that of the negative-parity $\nu h_{11/2}[532]5/2^-$ orbital, and due to the uncertainties inherent in PES calculations, the ground-state configuration for ^{117}Ba cannot be predicted reliably. As mentioned earlier, the ground state of ^{117}Ba was suggested to be a $I^\pi = 3/2^+$ state with a $\nu g_{7/2}[411]3/2^+$ configuration. A rotational band built on this configuration is populated weakly in the odd-A Ba isotopes, and was only observed in ^{121}Ba so far [18]. Hence, band 2 is interpreted as based on the $\nu d_{5/2}[413]5/2^+$ configuration.

Cranked shell model (CSM) calculations were performed in order to interpret the rotational behavior observed in ^{117}Ba . The deformation parameters (β_2, β_4, γ) were determined in total Routhian surface calculations [42, 43] and then used as input for CSM calculations [44] from which theoretical quasiparticle alignment frequencies can be extracted to be compared with the experimental values. The total Routhian has well-defined parity and signature, but no other quantum numbers are conserved. For the negative-parity band, at a rotational frequency $\hbar\omega = 0.15$ MeV, the $\alpha = -1/2(+1/2)$ signature is predicted to be characterised by deformation parameters of $\beta_2 \simeq 0.27(0.29)$, $\beta_4 \simeq 0.05(0.07)$, and $\gamma \simeq -9.8^\circ(2.2^\circ)$. For the positive-parity band at the same rotational frequency, the $\alpha = -1/2(+1/2)$ signature is calculated to have $\beta_2 \simeq 0.28(0.28)$, $\beta_4 \simeq 0.07(0.07)$, and $\gamma \simeq -3.0^\circ(-0.23^\circ)$. With these deformation parameters, CSM calculations indicate that the alignment of the first $h_{11/2}$ neutron (EF) and proton (ef) pairs occur at rotational frequencies of $\hbar\omega \simeq 0.42$ and 0.38 MeV, respectively, as presented in Fig. 8.

Since band 1 is proposed to be based on the $\nu h_{11/2}[532]5/2^-$ configuration, the first $h_{11/2}$ neutron (EF) alignment is blocked. The following EH (FG) alignment is calculated to occur at a crossing frequency above 0.6 Me; e.g., much higher than the experimental value. Thus, a neutron alignment is ruled out for this band. A proton ef alignment is expected to be responsible for the band crossing. The calculated proton (ef) crossing frequency $\hbar\omega \simeq 0.38$ MeV is consistent with the experimental results, and the observed large aligned angular momentum ($\sim 6.5 \hbar$ for both signatures) agrees well with the alignment of a pair of $\Omega = 1/2$, $h_{11/2}$ quasi-protons. Similar to the situation in $^{119,121}\text{Ba}$ [9, 18], a slight difference in alignment frequencies in the two signatures has been observed. This can presumably be attributed to a difference in their deformation as indicated in the CSM calculations. However, other scenarios, like an unpaired Landau-Zener-like crossing with a very different quasiparticle configuration, may also be at play and cannot be ruled out. But their roles cannot be pinned down by the present experimental data.

Both signatures of band 2 experience smooth gains in alignment in the observed frequency range (Fig. 7). The band crossing in the positive-parity band was system-

atically observed in heavier barium isotopes. For the $\alpha = -1/2$ signature, we note that the alignment becomes smoother with decreasing neutron number from ^{121}Ba to ^{119}Ba (see Fig. 5b in Ref. [18] and Fig. 6b in Ref. [9]). In ^{117}Ba , the alignment becomes even smoother than in ^{119}Ba , so that a band crossing frequency cannot be clearly identified. Based on the results of the CSM calculation, the alignment in band 2 could be attributed to the first proton (ef) alignment at $\hbar\omega = 0.38$ MeV or that of the first neutron (EF) at $\hbar\omega = 0.42$ MeV or a superposition of both, as there is no blocking effect for the $\nu d_{5/2}$ configuration. The $\alpha = -1/2$ signature reveals a large alignment gain of approximately $9 \hbar$ at measured frequency $\hbar\omega = 0.45$ MeV. This might indicate that the alignments in this signature consist of a superposition of proton ef and neutron EF alignments. In fact, a proton ef alignment superimposed or followed immediately by the neutron EF one was reported previously in ^{119}Ba and ^{121}Ba with a gain of $\sim 9 \hbar$ [9, 18]. The $\alpha = +1/2$ signature reveals an upbend at $\hbar\omega = 0.35$ MeV. This is due to the first pair of $h_{11/2}$ protons aligning, as the neutron EF alignment is predicted to occur at a somewhat higher frequency ($0.42 \text{ MeV}/\hbar$).

IV. SUMMARY

Using the Recoil-Decay Tagging technique, excited states in ^{117}Ba were identified and observed to high spins for the first time. Prompt γ rays belonging to ^{117}Ba were correlated with β -delayed protons from ^{117}Ba . A level scheme consisting of one negative-parity and one positive-parity band was established, extending present knowledge of rotational bands to this neutron-deficient barium isotope yet. The $\nu h_{11/2}[532]5/2^-$ and $\nu d_{5/2}[413]5/2^+$ quasineutron configurations were proposed for the negative- and positive-parity bands, respectively, based on the existing level spacing systematics in the heavier odd-A barium isotopes. Additionally, the $I^\pi = 3/2^+$ state, connected to the positive-parity band in this experiment, was tentatively suggested to be the ground state of ^{117}Ba with a possible $\nu g_{7/2}[411]3/2^+$ configuration. These quasineutron configuration assignments were supported by PES calculations. The experimentally observed rotational behaviour in both negative- and positive-parity bands were interpreted within the CSM. It is found that the two bands in ^{117}Ba fit well into the systematics of the barium isotopic chain.

This work demonstrates the feasibility of performing a high-spin study of ^{117}Ba by using β -delayed proton decays as a tag. This opens up the possibility to perform γ -spectroscopy experiments for very neutron-deficient nuclei which exhibit β -delayed proton emission [45, 46].

V. ACKNOWLEDGEMENTS

This work was supported by the National Natural Science Foundation of China (Grant Nos. 11405224, 11435014, 11675225, U1632144, 11205208, and 11505035), and the ‘100 Talented Project’ of the Chinese Academy of Sciences, and the United Kingdom Science and Technology Facilities Council. This material is based upon work supported by the U.S. Department of Energy, Office of Science, Office of Nuclear Physics under Contract numbers DE-AC02-06CH11357. This research used resources of ANL’s ATLAS facility, which is a DOE Office of Science User Facility.

TABLE I: Gamma-ray transition energies, relative intensities, and proposed assignments in ^{117}Ba .

$E_\gamma(\text{keV})^a$	I_γ	$I_i^\pi \rightarrow I_f^\pi^b$
Band 1		
46.6		$(7/2^-) \rightarrow (5/2^-)$
55.3		$(11/2^-) \rightarrow (9/2^-)$
60.3		$(15/2^-) \rightarrow (13/2^-)$
123.6	$\geq 44(18)$	$(9/2^-) \rightarrow (7/2^-)$
169.9	$\geq 60(22)$	$(9/2^-) \rightarrow (5/2^-)$
178.4	$\geq 135(44)$	$(11/2^-) \rightarrow (7/2^-)$
287.3	56(22)	$(13/2^-) \rightarrow (11/2^-)$
342.2	87(54)	$(13/2^-) \rightarrow (9/2^-)$
347.7	334(130)	$(15/2^-) \rightarrow (11/2^-)$
435.2	40(19)	$(17/2^-) \rightarrow (15/2^-)$
495.0	66(10)	$(17/2^-) \rightarrow (13/2^-)$
515.4	268(58)	$(19/2^-) \rightarrow (15/2^-)$
616.2	84(37)	$(21/2^-) \rightarrow (17/2^-)$
646.4	251(49)	$(23/2^-) \rightarrow (19/2^-)$
702.2	64(17)	$(25/2^-) \rightarrow (21/2^-)$
708.3	66(18)	$(33/2^-) \rightarrow (29/2^-)$
723.6	68(18)	$(29/2^-) \rightarrow (25/2^-)$
745.4	222(23)	$(27/2^-) \rightarrow (23/2^-)$
779.2	64(18)	$(37/2^-) \rightarrow (33/2^-)$
810.7	157(46)	$(31/2^-) \rightarrow (27/2^-)$
837.4	138(40)	$(35/2^-) \rightarrow (31/2^-)$
847.3	116(36)	$(39/2^-) \rightarrow (35/2^-)$
869.6	54(16)	$(41/2^-) \rightarrow (37/2^-)$
905.8	88(29)	$(43/2^-) \rightarrow (39/2^-)$
973.8	79(27)	$(47/2^-) \rightarrow (43/2^-)$
Band 2		
87.9	$\geq 106(43)$	$(5/2^+) \rightarrow (3/2^+)$
124.2	$\geq 97(44)$	$(7/2^+) \rightarrow (5/2^+)$
169.2	114(25)	$(9/2^+) \rightarrow (7/2^+)$
180.0	29(15)	$(11/2^+) \rightarrow (9/2^+)$
211.9	$\geq 76(29)$	$(7/2^+) \rightarrow (3/2^+)$
221.3	19(9)	$(15/2^+) \rightarrow (13/2^+)$
235.3	45(15)	$(13/2^+) \rightarrow (11/2^+)$
250.7	20(8)	$(19/2^+) \rightarrow (17/2^+)$
291.0	32(11)	$(17/2^+) \rightarrow (15/2^+)$
293.3	88(46)	$(9/2^+) \rightarrow (5/2^+)$
338.3	22(12)	$(21/2^+) \rightarrow (19/2^+)$
349.3	222(58)	$(11/2^+) \rightarrow (7/2^+)$
416.0	77(30)	$(13/2^+) \rightarrow (9/2^+)$
456.7	100(8)	$(15/2^+) \rightarrow (11/2^+)$
512.4	61(8)	$(17/2^+) \rightarrow (13/2^+)$
542.3	96(28)	$(19/2^+) \rightarrow (15/2^+)$
588.8	76(30)	$(21/2^+) \rightarrow (17/2^+)$
617.2	83(24)	$(23/2^+) \rightarrow (19/2^+)$
649.4	63(15)	$(25/2^+) \rightarrow (21/2^+)$
686.3	78(23)	$(27/2^+) \rightarrow (23/2^+)$
690.9	61(28)	$(29/2^+) \rightarrow (25/2^+)$
751.6	72(30)	$(31/2^+) \rightarrow (27/2^+)$
818.5	71(26)	$(35/2^+) \rightarrow (31/2^+)$
871.9	42(20)	$(39/2^+) \rightarrow (35/2^+)$
916.8	36(19)	$(43/2^+) \rightarrow (39/2^+)$

^aEnergies are accurate to 0.5 keV for strong transitions. The errors increase to 1.0 keV for weaker ones (relative intensity $I_\gamma \leq 50$).

^bProposed spin and parity assignments for the initial I_i^π and final I_f^π levels.

-
- [1] W. R. Phillips, I. Ahmad, H. Emling, R. Holzmann, R. V. F. Janssens, T. -L. Khoo, and M. W. Drigert, *Phys. Rev. Lett* **57** 3257 (1986).
- [2] J. F. Smith, C. J. Chiara, D. B. Fossan, G. J. Lane, J. M. Sears, I. Thorslund, I. M. Hibbert, R. Wadsworth, I. Y. Lee, and A. O. Macchiavelli, *Phys. Lett. B* **483** 7 (2000).
- [3] J. F. Smith, C. J. Chiara, D. B. Fossan, G. J. Lane, J. M. Sears, I. Thorslund, H. Amro, C. N. Davids, R. V. F. Janssens, D. Seweryniak, I. M. Hibbert, R. Wadsworth, I. Y. Lee, and A. O. Macchiavelli, *Phys. Rev. C* **57** R1037 (1998).
- [4] X. C. Chen, J. Zhao, C. Xu, H. Hua, T. M. Shneidman, S. G. Zhou, X. G. Wu, X. Q. Li, S. Q. Zhang, Z. H. Li, W. Y. Liang, J. Meng, F. R. Xu, B. Qi, Y. L. Ye, D. X. Jiang, Y. Y. Cheng, C. He, J. J. Sun, R. Han, C. Y. Niu, C. G. Li, P. J. Li, C. G. Wang, H. Y. Wu, Z. H. Li, H. Zhou, S. P. Hu, H. Q. Zhang, G. S. Li, C. Y. He, Y. Zheng, C. B. Li, H. W. Li, Y. H. Wu, P. W. Luo, and J. Zhong, *Phys. Rev. C* **94** 021301(R) (2016).
- [5] R. Wyss, A. Granderath, R. Bengtsson, P. von Brentano, A. Dewald, A. Gelberg, A. Gizon, J. Gizon, S. Harissopulos, A. Johnson, W. Lieberz, W. Nazarewicz, J. Nyberg, and K. Schiffer, *Nucl. Phys. A* **505** 337 (1989).
- [6] Hua-Lei Wang, Jie Yang, Min-Liang Liu, and Fu-Rong Xu, *Phys. Rev. C* **92** 024303 (2015).
- [7] R. Ma, Y. Liang, E. S. Paul, N. Xu, D. B. Fossan, L. Hildingsson, and R. A. Wyss, *Phys. Rev. C* **41** 717 (1990), and references therein.
- [8] A. P. Byrne, K. Schiffer, G. D. Dracoulis, B. Fabricius, T. Kibédi, A. E. Stuchbery, and K. P. Lieb, *Nucl. Phys. A* **548** 131 (1992).
- [9] J. F. Smith, C. J. Chiara, D. B. Fossan, G. J. Lane, J. M. Sears, I. Thorslund, H. Amro, C. N. Davids, R. V. F. Janssens, D. Seweryniak, I. M. Hibbert, R. Wadsworth, I. Y. Lee, A. O. Macchiavelli, A. V. Afanasjev, and I. Ragnarsson, *Phys. Rev. C* **61** 044329 (2000).
- [10] A. Al-Khatib, A. K. Singh, H. Hübel, P. Bringel, A. Bürger, J. Domscheit, A. Neußer-Neffgen, and G. Schönwaßer, et al., *Phys. Rev. C* **74** 014305 (2006).
- [11] P.-H. Heenen, J. Skalski, P. Bonche, and H. Flocard, *Phys. Rev. C* **50** 802 (1994).
- [12] J. F. Smith, C. J. Chiara, D. B. Fossan, D. R. LaFosse, G. J. Lane, J. M. Sears, K. Starosta, M. Devlin, F. Lerma, D. G. Sarantites, S. J. Freeman, M. J. Leddy, J. L. Durell, A. J. Boston, E. S. Paul, A. T. Semple, I. Y. Lee, A. O. Macchiavelli, and P. H. Heenen, *Phys. Lett. B* **523** 13 (2001).
- [13] G. de Angelis, A. Gadea, E. Farnea, R. Isocrate, P. Petkov, N. Marginean, D. R. Napoli, A. Dewald, M. Bellato, A. Bracco, F. Camera, D. Curien, M. De Poli, E. Fioretto, A. Fitzler, S. Kasemann, N. Kintz, T. Klug, S. Lenzi, S. Lunardi, R. Menegazzo, P. Pavan, J. L. Pedroza, V. Pucknell, C. Ring, J. Sampson, and R. Wyss, *Phys. Lett. B* **535** 93 (2002).
- [14] J. DeGraaf, M. Cromaz, T. E. Drake, V. P. Janzen, D. C. Radford, and D. Ward, *Phys. Rev. C* **58** 164 (1998).
- [15] Z. Liu, X. Sun, X. Zhou, X. Lei, Y. Guo, Y. Zhang, X. Chen, H. Jin, Y. Luo, S. X. Wen, C. X. Yang, G. J. Yuan, G. S. Li, X. A. Liu, W. D. Luo, and Y. S. Chen, *Eur. Phys. J. A* **1** 125 (1998).
- [16] Zhu Sheng-Jiang, M. Sakhaee, Yang Li-Ming, Gan Cui-Yun, Zhu Ling-Yan, Xu Rui-Qing, Jiang Zhuo, Zhang Zheng, Long Gui-Lu, Wen Shu-Xian, and Wu Xiao-Guang, *Chin. Phys. Lett* **18** 1027 (2001).
- [17] P. Mason, G. Benzoni, and A. Bracco, et al., *Phys. Rev. C* **72** 064315 (2005).
- [18] B. Cederwall, A. Johnson, R. Wyss, C.G. Lindén, S. Mitarai, J. Mukai, B. Fant, S. Juutinen, P. Ahonen, and J. Nyberg, *Nucl. Phys. A* **529** 410 (1991).
- [19] C. M. Petrache, G. Lo Bianco, D. Bazzacco, Th. Kröll, S. Lunardi, R. Menegazzo, M. Nespolo, P. Pavan, C. Rossi Alvarez, G. de Angelis, E. Farnea, T. Martinez, N. Marginean, D.R. Napoli, and N. Blasi, *Eur. Phys. J. A* **12** 135 (2001).
- [20] I. Y. Lee, *Nucl. Phys. A* **520** c641 (1990).
- [21] Cary N. Davids and James D. Larson, *Nucl. Instrum. Methods Phys. Res. B* **40/41** 1224 (1989); C. N. Davids, B. B. Back, K. Bindra, D. J. Henderson, W. Kutschera, T. Lauritsen, Y. Nagame, P. Sugathan, A.V. Ramayya, and W. B. Walters, **70** 358 (1991).
- [22] E. S. Paul, P. J. Woods, T. Davinson, R. D. Page, P. J. Sellin, C. W. Beausang, R. M. Clark, R. A. Cunningham, S. A. Forbes, D. B. Fossan, A. Gizon, J. Gizon, K. Hauschild, I. M. Hibbert, A. N. James, D. R. LaFosse, I. Lazarus, H. Schnare, J. Simpson, R. Wadsworth, and M. P. Waring, *Phys. Rev. C* **51** 78 (1995).
- [23] D. Seweryniak, M. P. Carpenter, S. Gros, A. A. Hecht, N. Hoteling, R. V. F. Janssens, T. L. Khoo, T. Lauritsen, C. J. Lister, G. Lotay, D. Peterson, A. P. Robinson, W. B. Walters, X. Wang, P. J. Woods, and S. Zhu, *Phys. Rev. Lett* **99** 022504 (2007).
- [24] P. Tidemand-Petersson, R. Kirchner, O. Klepper, E. Roeckl, D. Schardt, A. Płochocki, and J. Żylicz, *Nucl. Phys. A* **437** 342 (1985).
- [25] D. D. Bogdanov, A. V. Demyanov, V. A. Karnaukhov, L. A. Petrov, and J. Vobořil, *Nucl. Phys. A* **303** 145 (1978).
- [26] Z. Janas, L. Batist, J. Döring, M. Gierlik, R. Kirchner, J. Kurcewicz, H. Mahmud, C. Mazzocchi A. Płochocki, E. Roeckl, K. Schmidt, P. J. Woods, and J. Żylicz, *Eur. Phys. J. A* **23** 401 (2005).
- [27] Z. Liu, D. Seweryniak, P. J. Woods, C. N. Davids, M. P. Carpenter, T. Davinson, R. V. F. Janssens, R. D. Page, A. P. Robinson, J. Shergur, S. Sinha, X. D. Tang, and S. Zhu, *AIP Conf. Proc.* **961** 34 (2007).
- [28] Z. Liu, D. Seweryniak, P. J. Woods, C. N. Davids, M. P. Carpenter, T. Davinson, R. V. F. Janssens, R. D. Page, A. P. Robinson, J. Shergur, S. Sinha, X. D. Tang, F. R. Xu, and S. Zhu, *Phys. Lett. B* **702** 24 (2011).
- [29] P. Hornshøj, K. Wilsky, The ISOLDE Collaboration, CERN, Geneva, Switzerland, P. G. Hansen, B. Jonson, M. Alpsten, G. Andersson, Å. Appelqvist, B. Bengtsson, and O. B. Nielsen, *Phys. Lett. B* **34** 591 (1971).
- [30] D. C. Radford, *Nucl. Instrum. Methods Phys. Res. A* **361** 297 (1995).
- [31] F. Lidén, L. Hildingsson, Th. Lindblad, J. Gizon, D. Barnéoud, and J. Gascon, *Nucl. Phys. A* **524** 141 (1991).
- [32] K. Schiffer, A. P. Byrne, A. M. Baxter, G. D. Dracoulis, B. Fabricius, and A. E. Stuchbery, *Z. Phys. A* **336** 239 (1990).
- [33] J. Gizon and A. Gizon, *Z. Phys. A* **281** 99 (1977).
- [34] M. Shibata, H. Iimura, M. Asai, A. Osa, K. Kawade, S. Ichikawa, M. Oshima, T. Sekine, and N. Shinohara, *Phys.*

- Rev. C **65** 024305 (2002).
- [35] R. Wyss, F. Lidén, J. Nyberg, A. Johnson, D. J. G. Love, A. H. Nelson, D. W. Banes, J. Simpson, A. Kirwan, and R. Bengtsson, Z. Phys. A **330** 123 (1988).
 - [36] A. Dewald, A. Schmidt, G. Alexius, O. Vogel, R. S. Chakrawarthy, D. Bazzacco, P. von Brentano, A. Gizon, J. Gizon, S. Lunardi, D. R. Napoli, P. Pavan, C. Rossi Alvarez, and I. Wiedenhöver, Eur. Phys. J. A **3** 103 (1998).
 - [37] S. A. Wells, S. A. Wells, D. E. Evans, J. A. R. Griffith, D. A. Eastham, J. Groves, J. R. H. Smith, D. W. L. Tolfree, D. D. Warner, J. Billowes, I. S. Grant, and P. M. Walker, Phys. Lett. B **211** 272 (1988).
 - [38] A. C. Mueller, F. Buchinger, W. Klempt, E.W. Otten, R. Neugart, C. Ekström, and J. Heinemeier, Nucl. Phys. A **403** 234 (1983).
 - [39] R. Bengtsson and S. Frauendorf, Nucl. Phys. A **327** 139 (1979).
 - [40] Samuel M. Harris, Phys. Rev. **138** B509 (1965).
 - [41] F. R. Xu, P. M. Walker, J. A. Sheikh, and R. Wyss, Phys. Lett. B **435** 257 (1998).
 - [42] W. Nazarewicz, R. Wyss, and A. Johnson, Phys. Lett. B **225** 208 (1989).
 - [43] R. Wyss, J. Nyberg, A. Johnson, R. Bengtsson, and W. Nazarewicz, Phys. Lett. B **215** 211 (1989).
 - [44] W. Nazarewicz, J. Dudek, R. Bengtsson, T. Bengtsson, and I. Ragnarsson, Nucl. Phys. A **435** 397 (1985).
 - [45] B. Blank and M. J. G. Borge, Prog. Part. Nucl. Phys. **60** 403 (2008).
 - [46] S.-W. Xu, Z.-K. Li, Y.-X. Xie, Q.-Y. Pan, W.-X. Huang, X.-D. Wang, Y. Yu, Y.-B. Xing, N.-C. Shu, Y.-S. Chen, F.-R. Xu, and K. Wang, Phys. Rev. C **71** 054318 (2005).